Electrosprayed Janus particles for combined photo-chemo-therapy

Brenda Sanchez-Vazquez,[1] Adérito J. R. Amaral,[1] Deng-Guang Yu,[2]* George Pasparakis,[1]* and Gareth R. Williams[1]*

[1] UCL School of Pharmacy, 29-39 Brunswick Square, London, WC1N 1AX, UK.

[2] School of Materials Science & Engineering, University of Shanghai for Science and Technology, Shanghai 200093, China.

*Corresponding authors. E-mail: g.pasparakis@ucl.ac.uk (GP); ydg017@usst.edu.cn (DGY); g.williams@ucl.ac.uk (GRW).

Running head: Janus particles for **photo-chemo-therapy**

Abstract

This work is a proof of concept study establishing the potential of electrosprayed Janus particles for combined photodynamic therapy-chemotherapy. Sub-micron sized particles of polyvinylpyrrolidone containing either an anti-cancer drug (carmofur) or a photosensitiser (rose bengal; RB), and Janus particles containing both in separate compartments were prepared. The functional components were present in the amorphous form in all the particles, and infrared spectroscopy indicated that intermolecular interactions formed between the different species. *In vitro* drug release studies showed that both carmofur and RB were released at approximately the same rate, with dissolution complete after around 250 min. Cytotoxicity studies were undertaken on model human dermal fibroblasts (HDF) and lung cancer (A549) cells, and the influence of light on cell death explored. Formulations containing carmofur as the sole active ingredient were highly toxic to both cell lines, with or without a light treatment. The RB formulations were non-toxic to HDF when no light was applied, and with photo-treatment caused large amounts of cell death for both A549 and HDF cells. The Janus formulation containing both RB and carmofur was non-toxic to HDF without light, and only slightly toxic with the photo-treatment. In contrast it was hugely toxic to A549 cells when light was applied. The Janus particles are thus highly selective for cancer cells, and it is hence proposed that such electrosprayed particles containing both a chemotherapeutic agent and photosensitiser have great potential in combined chemotherapy/photodynamic therapy.

Keywords

Electrospraying; Janus particles; photodynamic therapy; chemotherapy.

Introduction

Photodynamic therapy (PDT) is a FDA (Food and Drug Administration) approved treatment for non-small cell lung cancer and esophageal cancer (1). It involves the application of a photosensitizer, an agent that generates cytotoxic reactive oxygen species (ROS) upon excitation with visible or near infrared light. Owing to the requirement for light-activation, PDT is a highly selective method which can be used to deliver a therapeutic dose localised only at the irradiated areas, and thus cancerous tissue can be treated without damaging healthy cells. In addition, the phototoxicity produced by PDT does not affect the collagen or elastin of the tissue and thus allows localised destruction of cancer cells with no long-term scarring or side effects (2).

More recently, the combination of anticancer drugs with photosensitisers in a single formulation has been explored as an aggressive means to synergise ROS-mediated cancer cell necrosis with the apoptotic events driven by chemotherapeutic agents (3-5). Although combinatorial photo-chemotherapeutic protocols have been successfully employed, and some are at pre-clinical stages (6, 7), there are still significant formulation challenges that need to be overcome: namely, the drug carrier must be capable of being co-loaded with two or more different compounds (*i.e.* the photosensitizer and the drug) which often exhibit completely different physicochemical properties (*e.g.* lipophilicity, molecular mass). Furthermore, the formulation should reach the target sites and release the molecular cargo at the desired tissue sites or cellular organelles with release profiles optimised to maximise the therapeutic effect (8). In order to fulfil these requirements, it is critical to develop new formulation methods capable of providing architectural compartmentalisation at the nano- to microscale in order to produce systems able to act as single platforms for multiple drug compounds in combinatorial cancer photo-chemo-therapies (9). **The Kataoka group have established the importance of such compartmentalisation in micellar formulations with a core-shell architecture, and elegantly demonstrated the protection of active biologics (DNA/RNA) from photo-oxidative damage during photochemical internalization (10, 11).**

Janus particles are anisotropic “two-faced” particles with different surface **features** on the two sides (12). **Such nano- or micro-scale formulations constitute an alternative design approach for the co-delivery of multiple APIs. They offer some potential benefits over core/shell materials, because in the Janus architecture both compartments are exposed to the external environment. This means that, for instance, particles could be fabricated with the two sides made of different polymers. A particle could thus be taken up by a cell and release the drug loading from each of the two sides at different rates or times. Alternatively, one side of the particle could selectively bind to a cell membrane while the other delivers a drug payload.**

The synthesis and fabrication of Janus particles has proved to be challenging (13). Although there are several methods which can be used to produce these particles, such as the self-assembly of block copolymers, lithography based masking/unmasking, phase separation, and controlled surface nucleation, these methods are often multiple-step, time-consuming, and difficult if not impossible to scale up (14). An attractive alternative route to Janus systems is electrodynamic atomisation (EHDA). This is a top-down and one-step process which can produce a wide range of micro- or nanostructures, using electrical energy. Typically, a polymer and functional component(s) (such as active pharmaceutical ingredients) are dissolved in a volatile solvent, which is then loaded into a syringe fitted with a metal tip (the spinneret). The solution is expelled from the syringe at a controlled rate towards a metal collector, and a large (kV) potential difference is applied between the two. This causes rapid evaporation of the solvent as the polymer solution travels towards the collector, and leads to micron-sized particles (electrospraying) or nanofibers (electrospinning), typically with the functional component amorphously distributed in the polymer matrix.

Most often, single-fluid EHDA is used to make monolithic fibres or particles (15, 16). However, by using a side-by-side spinneret – essentially two metal needle tips adjacent to one another and touching in the middle – it is possible to prepare Janus structures. Gupta and Wilkes first reported the fabrication of Janus fibers using side-by-side electrospinning with polyvinyl chloride/polyurethane and polyvinyl chloride)/polyvinylidiene fluoride in 2003 (17), but since then only a very limited number of additional studies have followed their initial work (18-21).

The setup required to create side-by-side structures from the electrospraying technique has been investigated in several articles. For instance, the possibility of controlling the size of Janus particles from 135 µm to 3 µm by means of varying the electric field has been reported by Sun *et al.* (22). In another example, the large-scale production of Janus particles with adjustable morphologies and structures was achieved by using an oppositely charged twin-head electrospraying set-up (23). This permitted the creation of Janus particles from two different solutions ejected through two separate nozzles at high voltages of opposite polarities; the two streams collide with each other after solvent evaporation and precursor gelation, producing a range of different heterostructures.

On the basis of the work described above, we hypothesised that Janus particles loaded with a chemotherapeutic drug and a photosensitiser may have great potential in PDT. To date, the use of Janus particles fabricated by EDHA techniques in photodynamic therapy has not been explored, and thus here we describe a proof of concept study in which we set out to demonstrate that it is possible to prepare such particles loaded with a model chemotherapeutic agent (carmofur, an antineoplastic agent, which can prevent, inhibit or halt tumour growth) and a photosensitiser (rose bengal, RB) in

two different compartments. In order to rapidly assess the utility of our formulations, we opted to use the fast-dissolving polymer polyvinylpyrrolidone (PVP) as the carrier matrix. The chemical structures of all three materials are given in Figure 1. PVP/carmofur, PVP/rose bengal, and Janus PVP/carmofur/rose bengal particles were prepared and fully characterised. Drug release studies were undertaken, and finally *in vitro* cell experiments performed to explore the effect of the formulations on both non-cancer and cancerous cells.

Experimental methods

Materials

Rose bengal (RB, 95% Dye) was purchased from Sigma-Aldrich, ethanol (96% v/v) from Fisher Scientific Ltd, and PVP (Mw 56 kDa) from Alfa Aesar. Carmofur (99%) was supplied by Cambridge Scientific. Phosphate buffered saline (PBS, pH 7.4) powder was obtained from Sigma-Aldrich.

Electrospraying

A 5 % w/v solution of PVP was prepared in ethanol and stirred until complete dissolution of the polymer **had** occurred. Additional solutions were also prepared consisting of 5 % w/v PVP and the desired amounts of RB and carmofur (see Table 1). The polymer solutions were then loaded into a 5 mL syringe (Terumo) fitted with a spinneret of **0.61 mm** internal diameter (Nordson EFD). Solutions were pumped at a flow rate of 0.5 mL h^{-1} using a syringe pump (KDS100, Cole Parmer). To prepare the Janus particles, a side-by-side spinneret comprising two 0.6 mm internal diameter spinnerets joined together was employed with two syringe pumps driving the fluids independently (both at a rate of 0.5 mL h^{-1}). A high voltage DC power supply (HCP 35-35000, FuG Elektronik) was used to apply a potential difference (15-17 kV; see Table 1) between the spinneret and a metal collector plate (30 x 20 cm) covered in aluminium foil placed 20 – 22 cm away (details are given in Table 1). Experiments were performed at temperatures of 24 – 27 °C and relative humidities in the range 36 – 39 %.

Characterisation

Scanning electron microscopy (SEM): The morphology of the materials produced was studied using a field emission scanning electron microscope (FEI Quanta 200F) connected to a secondary electron detector. Samples were adhered to an SEM stub with carbon-coated double-sided tape and sputter-coated with gold prior to measurement. The particle size distribution was determined from SEM micrographs, using the ImageJ software v**1.48** (National Institutes of Health, US) to **manually** measure the diameters of at least 100 particles. **The diameters of spherical particles were measured, and for elongated particles the shortest width was used to estimate their size.**

Fluorescence microscopy: An EVOS® FL Cell Imaging System (ThermoFisher Scientific) fitted with GFP and DAPI filters was used to acquire fluorescence microscopy images.

Differential scanning calorimetry (DSC)*:* Analysis was conducted using a Q2000 differential scanning calorimeter (DSC; TA Instruments). Approximately 2 – 5 mg of sample was placed inside a non-hermetically sealed aluminum pan (T130425, TA Instruments). DSC analysis was carried out from 0 - 140 or 200 °C, at a temperature ramp of 10 °C min^{-1} under a 50 mL min^{-1} flow of oxygen-free nitrogen gas. Data analysis was carried out using the TA Universal Analysis software.

X-ray diffraction (XRD) patterns were obtained using a Miniflex 600 (Rigaku) X-ray diffractometer supplied with Cu Kα radiation. Patterns were recorded over the 2Θ range 3 – 40° at a speed of 5° min^{-1}. The generator voltage was set at 40 kV and the current at 15 mA.

FT-IR spectroscopy: Fourier transform infrared spectroscopy was carried out using a Spectrum 100 FTIR spectrometer (PerkinElmer) in the range 500 − 4000 cm^{-1}, with a resolution of 4 cm^{-1} and accumulation of 16 scans.

Functional performance assays

Drug release was carried out in 250 mL of PBS (10 mM; pH 7.4) at a temperature of 37 °C. 10 mg of electrosprayed particles (PVP-RB, PVP-C, or PVP-RBC) were accurately weighed and placed in a capsule (Capsugel size 0, gelatine). The capsule was then placed in a sinker before being added to the dissolution medium. Experiments were conducted under continuous mechanical stirring at 100 rpm. Drug release was calculated on the basis of pre-determined calibration curves, obtained at wavelengths of 547 nm for rose bengal (24) and 259 nm for carmofur (25). PVP has no absorbance at these wavelengths, and the two active ingredients do not interfere with each other for quantification purposes.

Cell viability: The human dermal fibroblast (HDF) cell line was purchased from Life Technologies (lot 771555). The cells were maintained at 37 °C, under a 5% CO_2 atmosphere in Dulbecco's modified Eagle's medium-high glucose (DMEM-HG) supplemented with 10 % (v/v) heat-inactivated foetal bovine serum (FBS), 2 mM L-glutamine (Life Technologies), 1 % MEM non-essential amino acids, gentamicin solution (100 µg mL^{-1}) and amphotericin B solution (0.25 µg mL^{-1}). Cells were passaged when a confluence of 70 – 80 % was reached. This process involved a treatment with 0.05 % trypsin-EDTA solution and reseeding at a concentration of 1.5 x 10^5 cells mL^{-1}.

The lung cancer cell line A549 (ATCC CCL-185) was a kind gift from Dr Satyanarayana Somavarapu (UCL School of Pharmacy). The cells were maintained at 37 °C in a 5% CO_2 atmosphere in RPMI medium

(Gibco) supplemented with penicillin (100 µg mL^{-1}), streptomycin (100 µg mL^{-1}), L-glutamine (2 mM), and 10 % (v/v) heat-inactivated FBS (Gibco). The cells were passaged every 3 days and reseeded prior to use at a concentration of 9 x 10^5 cells mL^{-1}.

For assessment of the formulations, the materials to be tested were first dissolved in complete DMEM-HG or RPMI medium as appropriate to form solutions at 1 mg mL^{-1}. These were filtered through a 0.22 µm filter, and cells were directly resuspended in 180 µL of each solution in a 96-well plate (Greiner Bio-One Cellstar). Cell densities were 7.5 x 10^4 cells mL^{-1} for HDF and 5.5 x 10^4 cells mL^{-1} for A549. Doses of carmofur and RB in the controls were matched to their concentrations in the single-fluid particle solutions.

The cells were incubated with the dissolved formulations for 24 h, and then irradiated at 521 nm using a microscope illuminator (DiCon LED) for 20 min (1050 mW, 0.32 cm^2). Control experiments were also performed in which the cells were not exposed to light. Cell viability was determined using the CellTiter-Glo™ luminescent cell viability assay (Promega). The luminescent reagent was prepared following the manufacturer's instructions and added to the culture plates with a reagent volume equal to the volume of cell culture medium present in each well. After addition, the plate was left for 30 min at room temperature before luminescence was recorded using a SpectraMax M2e spectrophotometer (Molecular Devices). The viability of the cells was then calculated using the following formula:

$$\%\ viability\ = \frac{(Fluoresence\ of\ sample - background)}{(Fluoresence\ of\ control - background)} x\ 100$$

All experiments were performed in triplicate. Data from cell culture experiments are presented as mean ± standard deviation (S.D.) from three independent experiments, and were analysed using the SPSS Statistics Software. Statistical significance of differences was evaluated by one-way ANOVA using Games-Howell or Bonferroni *post hoc* tests. The level of significance was set at probabilities of $p < 0.001$ (***) and $p < 0.05$ (*).

Results

Particle morphology

SEM images of the particles prepared are given in Figure 2. The pure PVP particles have very regular spherical shapes, and the population is relatively monodisperse at 1.170 ± 0.162 µm. The addition of rose bengal to the formulation (PVP-RB) results in the production of some elongated particles, and a broadening of the size distribution (**0.537** ± **0.461** µm). **There are a large number of small particles at around 0.5 µm or below, with a smaller number of larger (> 1 µm) particles.** The carmofur-containing

(PVP-C) samples have more regular morphologies than PVP-RB, with the vast majority of the particles being spherical with smooth surfaces (Figure 2(c)). Only a few elongated particles can be observed, and the average diameter of the PVP-C particles **is 0.497 ± 0.209 µm**, similar to PVP-RB.

Janus particles were then prepared from side-by-side electrospraying with carmofur in one compartment and rose bengal in the other. These particles have rather irregular morphologies, with average size of 0.607 ± 0.191 µm. A central join or dimple is visible at the interface of the two sides, reflecting the characteristic compartmentalised architecture of the particles (Figure 2(d)). The dual-compartment structure of the particles is also very clear from the fluorescence microscopy images (Figure 2(e)), where a distinct fluorescent signal is visible from each compartment corresponding either to rose bengal (green) or to carmofur (red); a yellow hue in the middle is also visible where the two signals overlap.

Physical characterisation

The physical form of RB and carmofur in the **particles** was assessed by XRD and DSC, and the results are shown in Figure 3. Pure carmofur exists as a crystalline material, as is evidenced by the presence of a clear melting endotherm at *ca.* 115°C in DSC **(Figure 3(a))**. The DSC thermogram also shows degradation peaks at T > 125 °C. The carmofur XRD pattern contains myriad Bragg reflections, confirming its crystalline nature. Rose bengal shows no melting events over the temperature range studied by DSC (its melting point is reported to be > 300 °C), but its crystalline nature is clear from the XRD pattern (Figure 3(b)).

All the electrosprayed formulations are amorphous materials, with or without any functional component loaded. All the DSC thermograms show broad endotherms from approximately 40 – 130 °C, attributed to the loss of adsorbed water (PVP is known to be highly hygroscopic), with no melting events present **(Figure 3(a))**. There are no Bragg reflections visible by XRD, with only the broad humps typical of amorphous systems being present in the diffraction patterns **(Figure 3(b))**. **The absence of the carmofur melting endotherm in DSC and of the Bragg reflections from both carmofur and RB in the XRD patterns demonstrate that the active ingredients exist as amorphous solid dispersions in these formulations, as widely reported in the literature for electrosprayed systems (26).**

The interactions of RB and carmofur with the polymer were investigated by FT-IR spectroscopy. The spectra of the raw and fabricated materials are depicted in Figure 4. The spectra of the formulations appear to be a combination of the starting materials, and as expected, the major changes are observed in the carboxylate region of the spectrum. The C=O stretch of PVP is present at 1652 cm^{-1} , while rose bengal's carbonyl stretch can be seen at 1614 cm^{-1}; the shift of the carbonyl group to a lower

wavenumber in rose bengal is a result of the higher electronegativity of the halogen substituents (27). With the PVP-RB particles, a single carbonyl band is found at 1652 cm^{-1}. The PVP and rose bengal bands have thus merged, suggesting the presence of interactions (*e.g.* electrostatic forces) between the two components of the **particles**.

Carmofur shows a series of peaks at 1660 – 1750 cm^{-1} and a broad peak at 1501 cm^{-1}, which could all be attributable to C=O groups. The latter, together with a series of peaks between 1720 and 1750 cm^{-1}, can still be discerned in the PVP-C particles, but the peaks at 1665 and 1688 cm^{-1} have merged with the PVP C=O stretch to give a single peak at around 1650 cm^{-1}. The spectrum of the PVP-RBC particles looks very similar to the pure PVP data, presumably because of the small amounts of each drug present compared to the overall PVP content in the system. However, there is a distinctive broad peak from carmofur centred at 1735 cm^{-1} and the PVP C=O band is shifted to 1647 cm^{-1}, again likely to be a result of intermolecular interactions.

The phonon vibrations of the raw RB and carmofur materials are absent in all the electrosprayed particles, consistent with the lack of long-range order and amorphous physical form noted from XRD and DSC.

Drug release

Drug release profiles for the formulations are given in Figure 5. As expected for PVP-based systems, release occurs rapidly and plateaus after 250 min (*ca.* 4 h). This is rather slower than usually seen for PVP materials, which we ascribe to our use of a capsule as a container for the particles in these experiments. There is a significant burst release with > 25 % of the loaded drug being released within 25 min. While the release profiles of RB are essentially identical from both the monolithic and Janus systems, the formation of Janus particles appears to reduce the release extent of carmofur: the profile of the release plots are very similar, but the PVP-C **particles** release 95.9 ± 6.6 % of the drug loading after 350 min while the PVP-RBC **Janus particles** release only 66.8 ± 9.9 % in the same time interval. RB, used here as its disodium salt, is highly soluble in water (1 mg mL^{-1}), but carmofur is a poorly water-soluble drug (0.0273 mg mL^{-1}). The *in vitro* release profiles of carmofur were thus much more influenced by the size and shape of the particles. Attempts were made to analyse the data using the Korsmeyer-Peppas model, but it was found that this model does not provide a good fit to the experimental data.

Cytotoxicity studies

The cytotoxicity of the particles was evaluated on the normal HDF cell line, and on A549 (lung cancer) cells (see Figure 6). When HDF cells are exposed to the particles without light exposure (Figure 6(a)),

the viability of the cells treated with the PVP, PVP-RB and PVP-RBC particles is indistinguishable from the control of untreated cells. Cells treated with RB alone also show this high level of viability. As expected, the viability of cells treated with carmofur alone show significantly reduced viability (19.5 ± 9.2 %). Those incubated with the PVP-C system have a cell viability of around 43.8 ± 17.9 %. When the same experiment is repeated but with the cells exposed to light at 521 nm (Figure 6(b)), very high levels of cell death are seen with RB or carmofur alone, and also with PVP-C. However, viability is much higher with the PVP-RB and PVP-RBC systems, at 92.3 ± 13.7 % and 72.4 ± 11.8 % respectively (as compared to 100 % for the untreated cells or 91.1 ± 12.3 % for PVP particles).

The A549 cell line exhibits similar behaviour to the HDF cells in the absence of light. RB and PVP-RB lead to modest declines in viability, with values of 74.5 ± 15.1 % and 62.5 ± 8.2 % respectively. PVP-RBC gives viability very similar to pure PVP particles, at 83.9 ± 13.9 %. Incubation with carmofur or PVP-C results in virtually complete cell death (Figure 6(c)). The effect of light exposure was also explored on A459 cells (Figure 6(d)). The PVP and PVP-RB particles cause a moderate decline in viability, while RB alone reduces viability to *ca.* 30 %. Carmofur alone, PVP-C, and the Janus particles result in nearly quantitative cell death.

From these experiments, it is clear that the PVP-RBC particles are effective in the selective killing of cancer cells. We calculated a *selectivity index* for the formulations, defined as the viability of HDF cells with light exposure divided by the viability of A549 cells under the same conditions (Table 2). From Table 2, it is clear that PVP has minimal toxicity for both HDF and A549 cells under these conditions, and carmofur has essentially the same toxicity with both cell lines, killing virtually all the cells present. The PVP-RB and PVP-C systems are more selective for cancer cells, while in the presence of light RB alone is much more toxic to HDF cells than A549. In contrast, the PVP-RBC Janus system shows a very high level of selectivity, being almost 1500 times as toxic to cancer cells as normal cells.

Discussion

The characterisation results demonstrate that side by side electrospraying could effectively be used to create bi-compartmentalized particles combining a photosensitizer (rose bengal) and a cytotoxic drug (carmofur). We successfully produced sub-micron sized particles with homogenously spherical morphologies and relatively narrow size distributions. The active components are present in the amorphous physical form in the formulations, as expected since the electrospraying technique induces rapid solvent evaporation, which prevents re recrystallization of the molecules (28). Our work adds to the body of literature on side-by-side EHDA processes. Similar setups have been used to create complex formulations that have been successful in co-loading incompatible drugs (29), allowing

selective degradation of the compartments and controlled dual phase release kinetics (30), or long circulation nanocarriers, amongst others (31).

In terms of their cellular activity, the PVP-RBC and PVP-RB materials did not show any significant decrease in HDF cell viability compared to the PVP control when no light irradiation was applied. This is expected, since light exposure is essential for the generation of cytotoxic ROS and inducing irreversible photodamage to cellular organelles, as reported in other studies (1, 32). The application of light increased the toxicity of PVP-RB somewhat, while the PVP-C material is toxic to these cells even without light. This is expected: carmofur is a prodrug and its active degradation product, 5-fluorouracil, has poor selectivity towards tumours (33). The Janus particles caused only small amounts of HDF cell death, with or without exposure to light.

In the case of the **experiments performed without light in the** A549 cell line, **a decrease of ~25 – 40 % cell viability was observed with the RB and PVP-RB formulations; this is expected to be caused by the intrinsic cytotoxicity of RB (even without exposure to light) (34)**. **After light irradiation, PVP-RB causes very similar levels of cell death (*ca.* 30 %) as was observed with no light treatment. In contrast**, PVP-C, and PVP-RBC kill almost all the cells present. The PVP-RBC formulation shows a very high level of selectivity for cancerous cells, inducing 1500-fold more cell death than with the non-cancerous HDF cells. This effect could be a result of the combination of photodynamic therapy and chemotherapy, which is proven to result in a significant inhibition of tumour proliferation, increased induction of apoptosis, and damage to tumour vasculature (35-37). Khadir *et al.* have also suggested that enhanced cytotoxicity could be correlated with improved intracellular and nuclear delivery of the two drugs (38). **One of the key benefits of photodynamic therapy is its high selectivity for tumour cells due to the ability of the photosensitisers to accumulate in tumour tissue rather than in normal cells, further helping to improve the selectivity of PVP-RBC in this work (39).**

We thus demonstrate here that Janus particles prepared by electrospraying have great potential in combined **photo-chemo-therapy**, showing high selectivity for cancerous cells. For the purposes of proof-of-concept, the materials prepared in this work used PVP as the carrier. This polymer dissolves very rapidly upon addition to water, allowing rapid assessment of functional performance. Onward formulation will be required to develop practicable drug delivery systems, for instance by embedding the particles prepared here in a secondary polymer matrix, or by using alternative polymers to prepare the electrosprayed Janus particles. We will take the latter forward in our future work now that the concept of using such particles in **photo-chemo-therapy** has been proven.

Conclusions

The aim of this study was to develop a compartmentalized structure for combined photodynamic (PDT) and chemotherapeutic treatment of cancer. Electrospraying was used to generate sub-micron particles of polyvinylpyrrolidone containing either an anti-cancer drug (carmofur) or a photosensitiser for PDT (rose Bengal; RB), and also Janus structures containing both in separate compartments. The products were largely spherical particles, and in the Janus case two distinct sections can be seen. The functional components are present in the amorphous form, as demonstrated by X-ray diffraction and differential scanning calorimetry. IR spectroscopy indicated the presence of intermolecular interactions between the different components of the particles. Drug release from the formulations was rapid, reaching a maximum after around 250 min. *In vitro* cytotoxicity assays were performed in HDF and A549 cells. Formulations containing only RB as the active ingredient were non-toxic in the absence of light, but when light was provided proved similarly toxic to the normal HDF and cancerous A549 cells. Those containing carmofur were highly toxic to both cells lines regardless of the presence of light. The Janus formulations were non-toxic to HDF cells without light, and somewhat more toxic after light was provided. They caused the death of almost 100 % of the A549 cells after exposure to light, however. The Janus formulations are highly selective for cancerous cells, and thus electrosprayed Janus particles are expected to have great potential in **photo-chemo-therapy.**

Acknowledgements

This work was supported by the China National Science Foundation / UK Royal Society cost share international exchanges scheme (No. 51411130128/IE131748) and the National Science Foundation of China (No. 51373101), and we thank these bodies for funding. BSV would like to thank the Mexican Consejo Nacional de Ciencia y Tecnologia (CONACyT) for the provision of a PhD scholarship. GP thanks UCL for the award of an Excellence Fellowship and the EPSRC for financial support in the form of an Early Career Fellowship (EP/M014649/1).

References

1. Dolmans DE, Fukumura D, Jain RK. Photodynamic therapy for cancer. Nat Rev Cancer. 2003;3:380-7.
2. Webb CE, Jones JDC. Handbook of laser technology and applications: Laser design and laser systems. 1st ed. Baca Raton: CRC Press; 2004.
3. Pasparakis G, Manouras T, Vamvakaki M, Argitis P. Harnessing photochemical internalization with dual degradable nanoparticles for combinatorial photo–chemotherapy. Nat Commun. 2014;5:1:3623.
4. Lim E-K, Kim T, Paik S, Haam S, Huh Y-M, Lee K. Nanomaterials for Theranostics: Recent Advances and Future Challenges. Chem Rev. 2015;115:327-94.

5. Lee D-E, Koo H, Sun I-C, Ryu JH, Kim K, Kwon IC. Multifunctional nanoparticles for multimodal imaging and theragnosis. Chem Soc Rev. 2012;41:2656-72.
6. Agostinis P, Berg K, Cengel KA, Foster TH, Girotti AW, Gollnick SO, et al. Photodynamic therapy of cancer: An update. CA Cancer J Clin. 2011;61:250-81.
7. Huggett MT, Jermyn M, Gillams A, Illing R, Mosse S, Novelli M, et al. Phase I/II study of verteporfin photodynamic therapy in locally advanced pancreatic cancer. Br J Cancer. 2014;110:1698-704.
8. Pietroiusti A, Campagnolo L, Fadeel B. Interactions of Engineered Nanoparticles with Organs Protected by Internal Biological Barriers. Small. 2013;9:1557-72.
9. Kamaly N, Xiao Z, Valencia PM, Radovic-Moreno AF, Farokhzad OC. Targeted polymeric therapeutic nanoparticles: design, development and clinical translation. Chem Soc Rev. 2012;41:2971-3010.
10. Nomoto T, Fukushima S, Kumagai M, Machitani K, Arnida, Matsumoto Y, et al. Three-layered polyplex micelle as a multifunctional nanocarrier platform for light-induced systemic gene transfer. Nat Commun. 2014;5:3545.
11. Nishiyama N, Iriyama A, Jang W-D, Miyata K, Itaka K, Inoue Y, et al. Light-induced gene transfer from packaged DNA enveloped in a dendrimeric photosensitizer. Nat Mater. 2005;4:934-41.
12. Pang X, Wan C, Wang M, Lin Z. Strictly biphasic soft and hard Janus structures: synthesis, properties, and applications. Angew Chem Int Ed Engl. 2014;53:5524-38.
13. Walther A, Muller AHE. Janus particles. Soft Matter. 2008;4:663-8.
14. Perro A, Reculusa S, Ravaine S, Bourgeat-Lami E, Duguet E. Design and synthesis of Janus micro- and nanoparticles. J Mater Chem. 2005;15:3745-60.
15. Huang Z-M, Zhang YZ, Kotaki M, Ramakrishna S. A review on polymer nanofibers by electrospinning and their applications in nanocomposites. Compos Sci Technol. 2003;63:2223-53.
16. Zhang C-L, Yu S-H. Nanoparticles meet electrospinning: recent advances and future prospects. Chem Soc Rev. 2014;43:4423-48.
17. Gupta P, Wilkes GL. Some investigations on the fiber formation by utilizing a side-by-side bicomponent electrospinning approach. Polymer. 2003;44:6353-9.
18. Chen G, Xu Y, Yu DG, Zhang DF, Chatterton NP, White KN. Structure-tunable Janus fibers fabricated using spinnerets with varying port angles. Chemi Commun. 2015;51:4623-6.
19. Starr JD, Andrew JS. Janus-type bi-phasic functional nanofibers. Chem Commun. 2013;49:4151-3.
20. Starr JD, Budi MAK, Andrew JS. Processing-Property Relationships in Electrospun Janus-Type Biphasic Ceramic Nanofibers. J Am Ceram Soc. 2015;98:12-9.
21. Yu D-G, Yang C, Jin M, Williams GR, Zou H, Wang X, et al. Medicated Janus fibers fabricated using a Teflon-coated side-by-side spinneret. Colloids Surf B. 2016;138:110-6.
22. Sun X-T, Yang C-G, Xu Z-R. Controlled production of size-tunable Janus droplets for submicron particle synthesis using an electrospray microfluidic chip. RSC Adv. 2016;6:12042-7.
23. Mou F, Chen C, Guan J, Chen D-R, Jing H. Oppositely charged twin-head electrospray: a general strategy for building Janus particles with controlled structures. Nanoscale. 2013;5:2055-64.
24. Chang C-C, Yang Y-T, Yang J-C, Wu H-D, Tsai T. Absorption and emission spectral shifts of rose bengal associated with DMPC liposomes. Dyes Pigments. 2008;79:170-5.
25. Verma AK, Chanchal A, Maitra A. Co-polymeric hydrophilic nanospheres for drug delivery: release kinetics, and cellular uptake. Indian J Exp Biol. 2010;48:1043-52.
26. Williams GR, Chatterton NP, Nazir T, Yu DG, Zhu LM, Branford-White CJ. Electrospun nanofibers in drug delivery: recent developments and perspectives. Therap. Deliv. 2012;3:515-33.
27. Uppal A, Jain B, Gupta PK, Das K. Photodynamic action of Rose Bengal silica nanoparticle complex on breast and oral cancer cell lines. Photochem Photobiol. 2011;87:1146-51.
28. Lopez FL, Shearman GC, Gaisford S, Williams GR. Amorphous Formulations of Indomethacin and Griseofulvin Prepared by Electrospinning. Mol Pharm. 2014;11:4327-38.

29. Lai W-F, Susha AS, Rogach AL. Multicompartment Microgel Beads for Co-Delivery of Multiple Drugs at Individual Release Rates. ACS Appl Mater Interfaces. 2016;8:871-80.
30. Hwang S, Lahann J. Differentially degradable janus particles for controlled release applications. Macromol Rapid Commun. 2012;33:1178-83.
31. Rahmani S, Villa CH, Dishman AF, Grabowski ME, Pan DC, Durmaz H, et al. Long-circulating Janus nanoparticles made by electrohydrodynamic co-jetting for systemic drug delivery applications. J Drug Target. 2015;23:750-8.
32. Wilson BC. Photodynamic therapy for cancer: principles. Can J Gastroenterol. 2002;16:393-6.
33. Douglas KT. The thymidylate synthesis cycle and anticancer drugs. Med Res Rev. 1987;7:441-75.
34. Mousavi SH, Tavakkol-Afshari J, Brook A, Jafari-Anarkooli I. Direct toxicity of Rose Bengal in MCF-7 cell line: Role of apoptosis. Food Chem Toxicol. 2009;47:855-9.
35. Canti G, Nicolin A, Cubeddu R, Taroni P, Bandieramonte G, Valentini G. Antitumor efficacy of the combination of photodynamic therapy and chemotherapy in murine tumors. Cancer Lett. 1998;125:39-44.
36. Zhou L, Zhou L, Wei S, Ge X, Zhou J, Jiang H, et al. Combination of chemotherapy and photodynamic therapy using graphene oxide as drug delivery system. J Photochem Photobiol B. 2014;135:7-16.
37. Nonaka M, Ikeda H, Inokuchi T. Effect of combined photodynamic and chemotherapeutic treatment on lymphoma cells in vitro. Cancer Lett. 2002;184:171-8.
38. Khdair A, Chen D, Patil Y, Ma L, Dou QP, Shekhar MPV, et al. Nanoparticle-mediated combination chemotherapy and photodynamic therapy overcomes tumor drug resistance. J Control Release. 2010;141:137-44.
39. Plaetzer K, Krammer B, Berlanda J, Berr F, Kiesslich T. Photophysics and photochemistry of photodynamic therapy: fundamental aspects. Laser Med Sci. 2009;24:259-68.

Figures

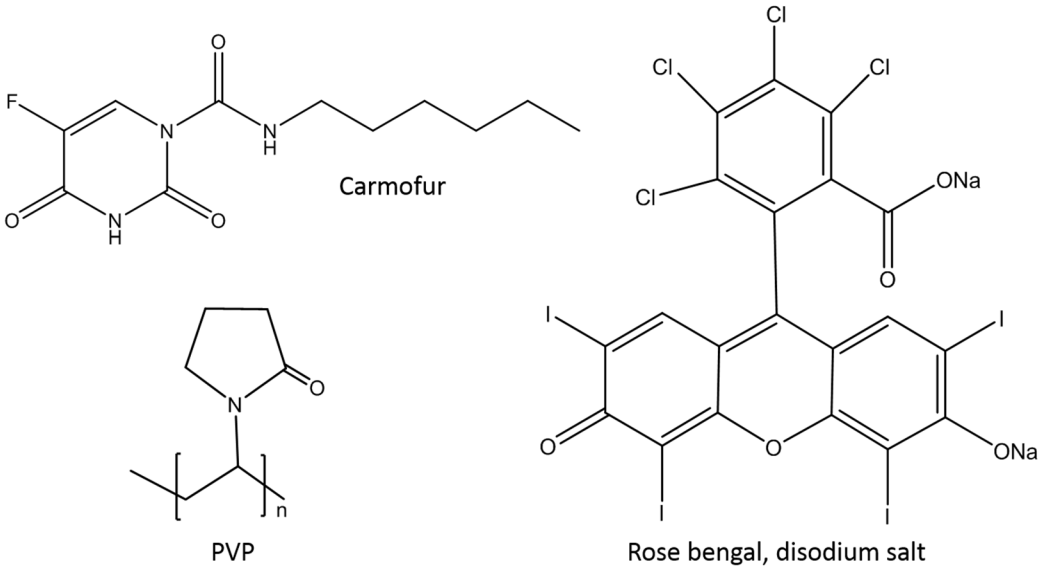

Figure 1. The chemical structures of PVP, carmofur and rose bengal.

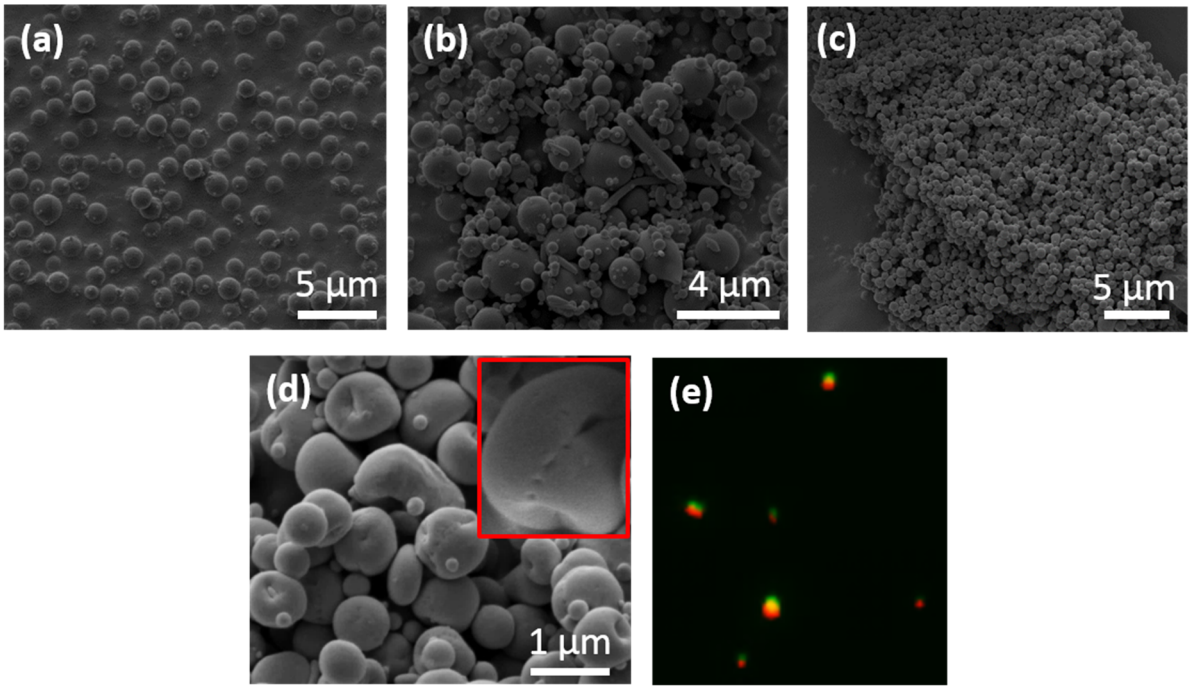

Figure 2. SEM images of electrosprayed (a) PVP; (b) PVP-RB; (c) PVP-C; and, (d) PVP-RBC particles, together with (e) a fluorescence micrograph of PVP-RBC.

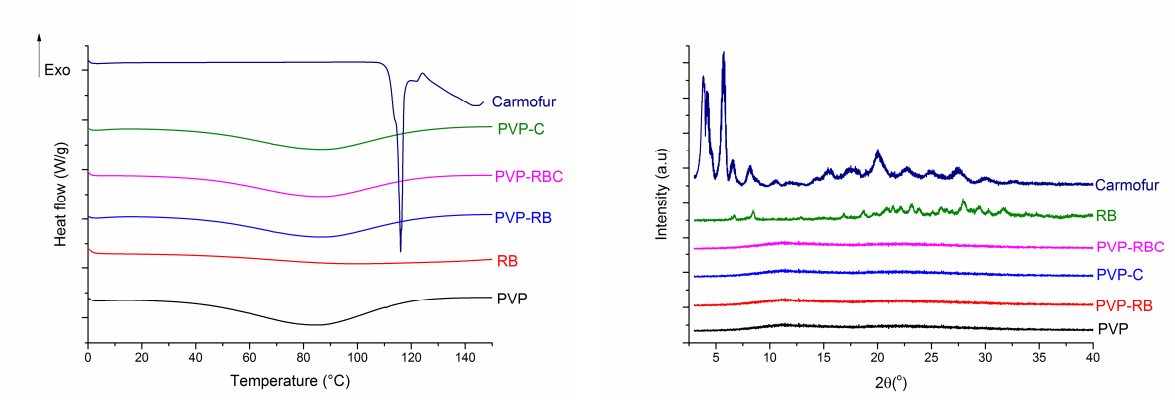

(a) (b)

441 Figure 3. Physical form characterization. (a) DSC and (b) XRD data are shown.
442

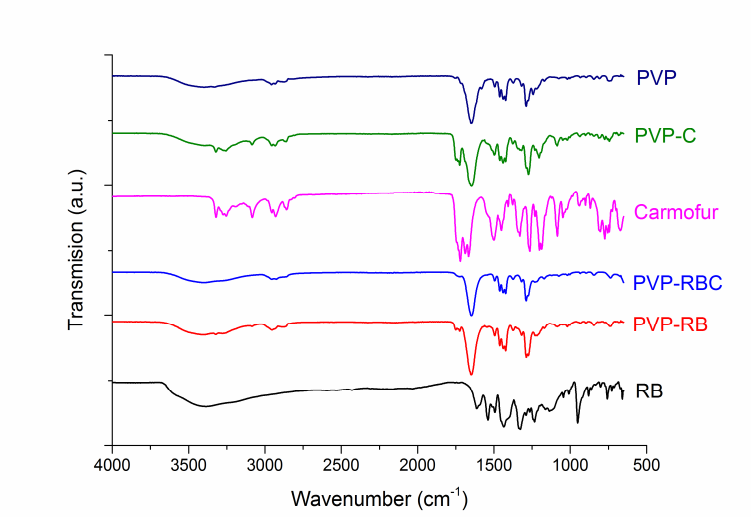

443
444 Figure 4. IR spectra of the raw materials and electrosprayed particles.
445

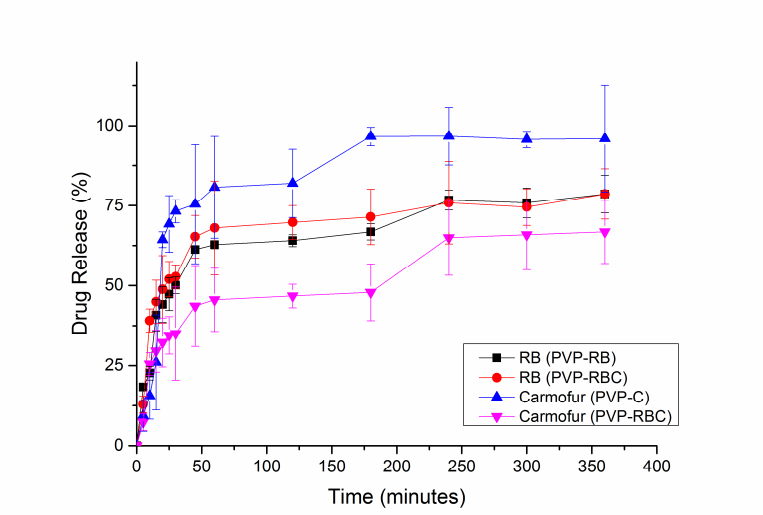

446
447 Figure 5. *In vitro* drug release from the electrosprayed particles. Data are given from three
448 independent experiments as mean ± S.D.
449

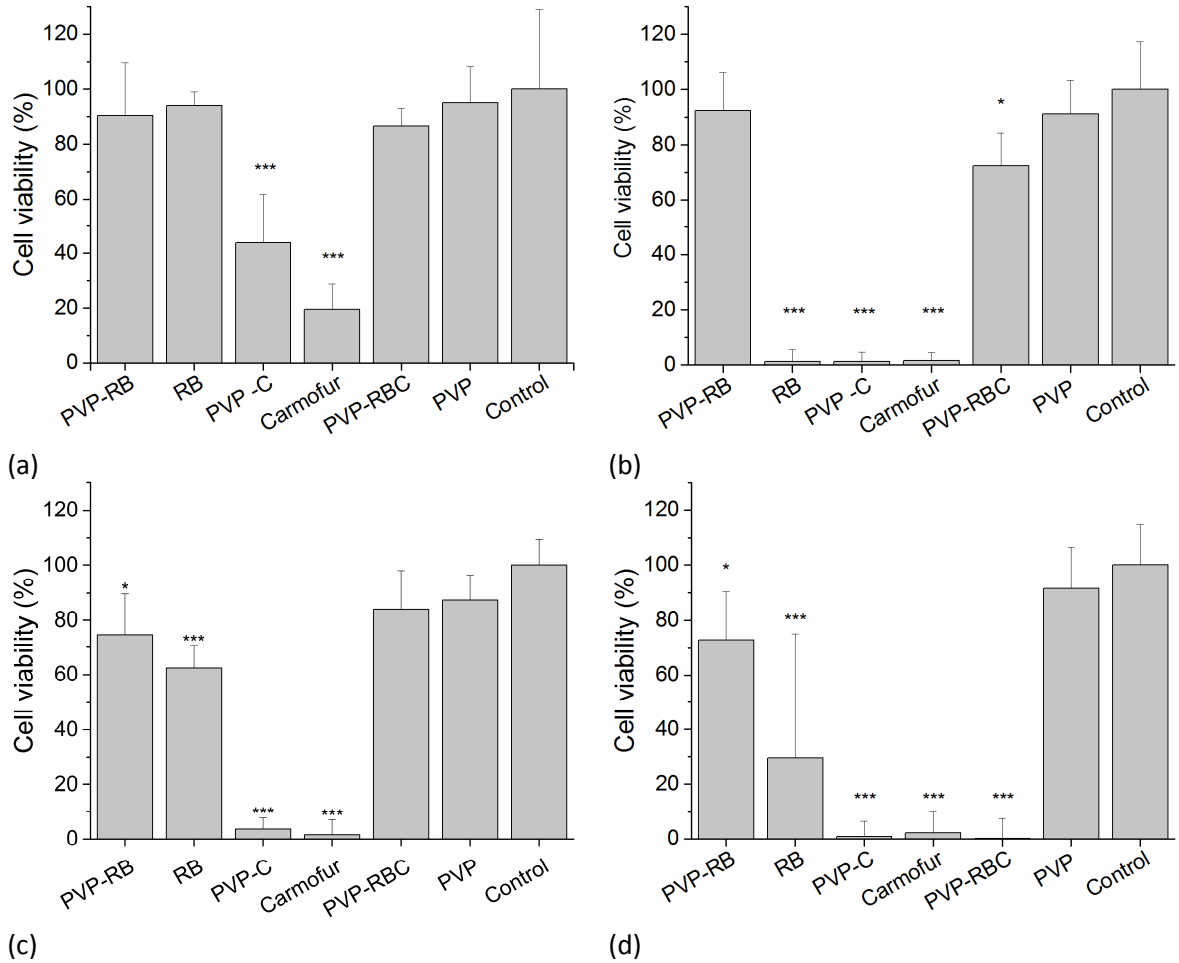

Figure 6. Cell viability studies with (a) HDF cells; (b) HDF cells exposed to light at 521 nm; (c) A549 cells and (d) A549 cells exposed to light at 521 nm. Data are shown from three independent experiments as mean ± S.D. *** denotes $p < 0.001$, and * $p < 0.05$ with respect to the control (untreated cells).

Tables

Table 1. Details of the working solutions used for electrospraying. The PVP-RBC particles were generated from a side-by-side spinneret using both the rose bengal and carmofur-containing solutions.

ID	Functional component(s)	Rose bengal conc. (% w/v)	Carmofur conc. (% w/v)	Collection distance (cm)	Voltage (kV)
PVP	-	-	-	22	15
PVP-RB	Rose bengal	0.10	-	22	15
PVP-C	Carmofur	-	0.86	22	15
PVP-RBC	Rose bengal and carmofur	0.10	0.86	20	17

Table 2. The selectivity of the formulations for cancer cells. The selectivity index is defined as the viability of HDF cells divided by the viability of the A549 cells. A value of > 1 indicates that the formulation is selective for cancerous cells.

ID	HDF viability (%)	A549 viability (%)	Selectivity index
PVP	91.1 ± 12.3	91.6 ± 14.8	0.99
PVP-RB	92.3 ± 13.7	72.8 ± 17.6	1.27
PVP-C	1.2 ± 3.5	0.85 ± 5.6	1.41
PVP-RBC	72.4 ± 11.8	0.05 ± 7.5	**1450**
RB	1.3 ± 4.2	29.4 ± 45.5	0.04
Carmofur	1.6 ± 3.0	2.16 ± 7.8	0.74